

effects. Potassium is an essential macroelement in plant nutrition as well as the most abundant cation in plant tissues. Plant growth and productivity demand high potassium doses for its consequent distribution throughout the plant (Marschner, 2011; Nieves-Cordones *et al.*, 2016).

However, there is a large knowledge gap in understanding the role of potassium fertilization in relation to drought resiliency in grapevines. The present investigation was driven by the hypothesis that abundant potassium levels enable grapevines' tolerance to drought periods and exposes actual evapotranspiration and canopy effects to explore grapevines' resilience to drought periods.

Materials and Methods

Experimental Setup

The experimental platform is located in the southern district of Israel, specifically in the northern region of the Negev desert at the Gilat Research Center for Arid & Semi-Arid Agricultural Research, Agricultural Research Organization— Volcani Institute of Israel's Ministry of Agriculture. The institution is situated at latitude 31° 20' N, longitude 34° 40' E, and approximately 150 m above sea level; Be'er Sheva city is 20 km away (Figure 1).

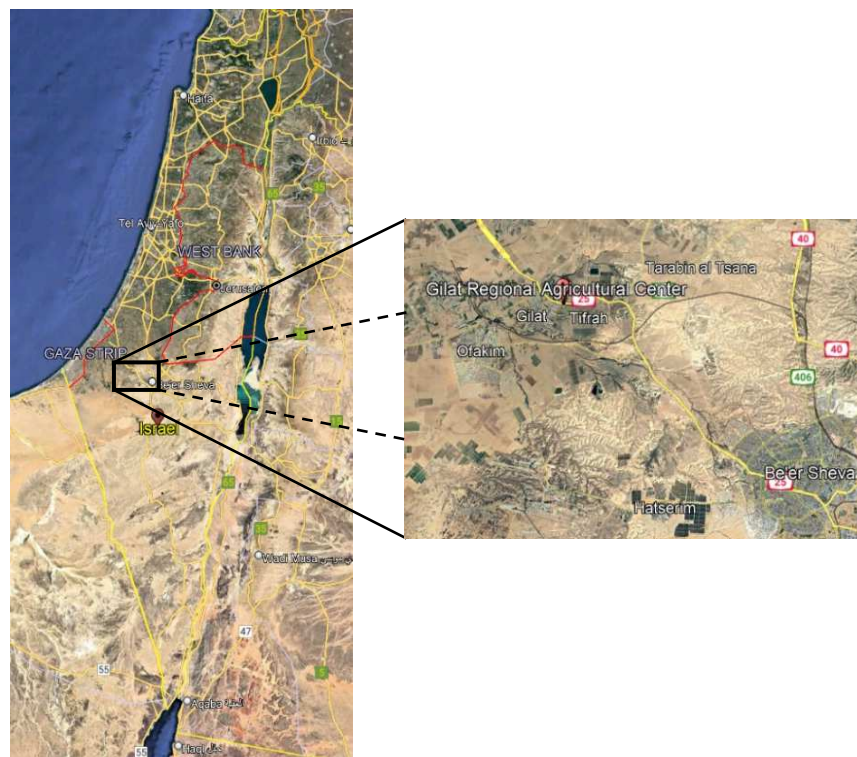


Figure 1. Location of the Gilat Research Center.

The climate of the experimental site based on the Köppen climate classification is defined as BWh, hot and dry summers, and mild winters. Precipitation is mainly concentrated in the winter season, being rare in summer (Potchter & Ben-Shalom, 2013). According to historical meteorological data of the Land Conservation Division of Israel's Ministry of Agriculture, in the station Gilat during the period 2008-2022, the average maximum temperature was 27.8°C (range of 35-18.5°C), August being the hottest month with an average maximum temperature of 35°C and an average minimum of 21.7°C. Likewise, the average minimum temperature was 14.5°C (range of 21.7-7.8°C), January being the coldest month with an average maximum temperature of 18.5°C and an average minimum temperature of 7.8°C. The average annual temperature was 21.2 °C (Agrometeo, 2023).

Experimental Design

The research comprised weighing lysimeter experimentation to evaluate potassium concentration effects in physiological development response under short drought stress periods in Early Sweet (var) grapevines (*Vitis vinifera* cv.). The experiment was conducted in an experimental set-up with twenty-eight weighing lysimeters; however, just twenty-four were working properly. In the present research, for data management reasons, a single random tree was selected per treatment for ET_a rates analysis while for canopy were used twenty-four grapevines; every lysimeter contained a single grapevine tree.

In March 2018, the grapevines (“Early Sweet” grafted on “140 Ruggeri”) were planted in 10L pots. In March 2020, they were transplanted to the weighing lysimeters. The trees were distributed homogeneously in four rows of seven lysimeters, the separation between trees was 2.5 m and between rows 5 m.

Six treatments were randomly allocated and established based on three potassium levels and two irrigation regimes (Appendix 1), as described below:

1. Well-watered grapevine with 60 mg K⁺ L⁻¹ (60WW)
2. Well- watered grapevine with 15 mg K⁺ L⁻¹ (15WW)
3. Well- watered grapevine with 5 mg K⁺ L⁻¹ (5WW)
4. Water-deficit grapevine with 60 mg K⁺ L⁻¹ (60WD)
5. Water-deficit grapevine with 15 mg K⁺ L⁻¹ (15WD)
6. Water-deficit grapevine with 5 mg K⁺ L⁻¹ (5WD)

The well-watered treatments integrated approximately 130-140% water from last-day actual evapotranspiration. In contrast, in water-deficit treatments, the grapevines were dehydrated by interrupting irrigation during episodic drought trials until reaching critical physiological values based on stomatal conductance and stem water potential (see drought trials).

Grapevines were fertigated daily with mineral fertilizers through drip irrigation, varying the potassium concentration depending on the experimental treatment (60, 15, 5 mg K⁺ L⁻¹) at 40 mg N L⁻¹, 10 mg P L⁻¹, 35 mg Ca L⁻¹, 15 mg Mg L⁻¹, 0.025 mg Cu L⁻¹, 0.6 mg Fe L⁻¹, 0.3 mg Mn L⁻¹, 0.016 mg Mo L⁻¹, and 0.15 mg Zn L⁻¹, following Israeli commercial vineyard management (Hochberg *et al.*, 2023).

Lysimeter Experimentation

Weighing lysimeters were composed of polyethylene containers with a volume of 2 m³ (1.4 m diameter and 1.3 m high), four load-cells brand Zemic Europe B.V model H8C-C3-2.0T-4B in parallel, and a metal platform (Hochberg *et al.*, 2023). The lysimeter's containers were filled with loamy sand soil (88-95% sand and 4-10% clay) (*ibid.*) The excess of water was drained by an inert rockwool extension to 50 L buckets at one meter below the soil container bottom (Ben-Gal & Shani, 2002; Hochberg *et al.*, 2023). Drainage water accumulated in the collection buckets was automatically emptied through an electric valve. As the bucket was connected to the weighing lysimeter, measurement of lysimeter mass before and after its emptying indicated volume of the drainage. A drip irrigation line was installed per lysimeter with 16mm pipeline diameter, and eight pressure-compensated drip emitters of 2.0 L h⁻¹ model PC online, brand Netafim Tel Aviv. Grapevines grew vertically to 1.2 m height supported by a commercial Y-shaped trellis with dimensions of 1.4 by 2.7 m (Figure 2) (Hochberg *et al.*, 2023). The group of lysimeters included an automatic water and fertilizer preparation and delivery system (Ben-Gal *et al.*, 2010).

Lysimeter mass data was collected and stored in a field-installed data logger and automatically downloaded to a comma-separated Excel file through a preprogrammed digital interface (LoggerNet 4.7, Campbell Scientific) using a main project PC located in the research center offices. Likewise, the lysimeters were calibrated on-field with a known mass (< 50 kg) before each drought trial through the mentioned interface and the project's main PC using the AnyDesk application and mobile data (in order to use the main PC remotely); the admissible percentage error in the calibration (known mass concerning measured mass) was defined as $\pm 2\%$.

The data collection system in the lysimeters was programmed to measure mass at five-minute intervals and considering the expected mass changes in a day (relative mass ranging from approximately -100 to 100 kg). The main objective of using weighing lysimeters was to calculate the actual daily evapotranspiration through a water balance, considering the mass of the irrigation, drainage, and change in water storage components (see data collection section) (Ben-Gal *et al.*, 2010). Appendix 2 shows schemes elaborated in AutoCAD 2023 that highlight the components of the weighing lysimeters used in the present investigation (front, side, and top view).

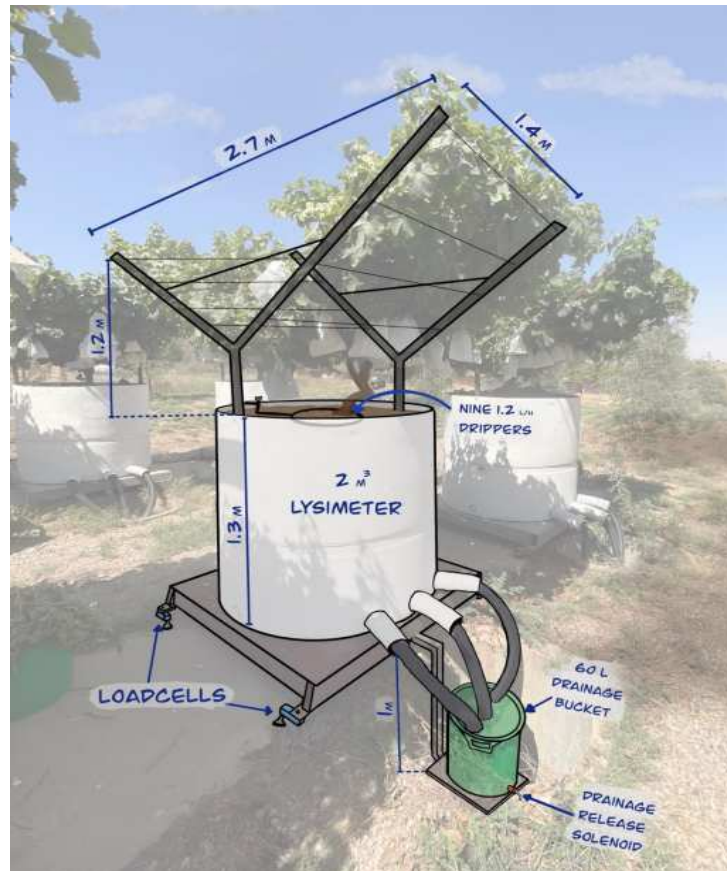


Figure 2. Lysimeter setup at Gilat Research Center, ARO-Volcani Institute, Israel (Hochberg *et al.*, 2023).

Drought Trials

In the present investigation, two drought trials were carried out. The trials were monitored daily considering daily actual evapotranspiration and two physiological parameters to monitor critical water status: stomatal conductance and stem water potential (see data collection section). In the case of grapevines, a severe water deficit was defined when the midday stomatal conductance was approximately equal to or greater than $0.02 \text{ mol m}^{-2} \text{ s}^{-1}$ and stem water potential was approximately -1.0 to -1.2 MPa (Flexas *et al.*, 2002; Hochberg *et al.*, 2023).

The drought trials comprised irrigation interruption, inducing the dehydration of the plant until reaching a severe water deficit based on the mentioned physiological parameters. The critical drought point was maintained for some days by supplying daily small amounts of water equal to the previous day's stress level ET_a . Subsequently, the irrigation was re-established for the vine recovery, and measurements continued until reaching the same values in both physiological parameters as the well-irrigated homologous treatments (Hochberg *et al.*, 2023).

The first drought trial was carried out from April 28th to May 11th, 2023 (1st third of the crop cycle), and the second from June 8th to 18th, 2023 (between 2nd and 3rd third of the crop cycle). The critical drought days in the first drought were May 10th and 11th, 2023, while the second

were from June 14th to 18th, 2023. The vine rehydration (or recovery) in the first drought comprised from May 12th to 17th, 2023, and the second from June 19th to 23rd, 2023.

Estimation of Diurnal Actual Evapotranspiration (ET_a)

The diurnal ET_a was calculated using the water balance method concerning the period of the day in which this process is encouraged. From a whole-tree daily ET_a perspective, it must be considered the irrigation supply, drainage, and change in soil water storage, as depicted in the following equation:

$$ET_{a-d} = I - D - \Delta S \quad (1)$$

Where ET_{a-d} is daily actual evapotranspiration ($L \text{ tree}^{-1} \text{ day}^{-1}$), I is irrigation (L), D is drainage (L), and ΔS is change in soil water storage (L) (Ben-Gal *et al.*, 2010; Hochberg *et al.*, 2023) (Equation 1). Figure 3 illustrates the water balance components, as well as the behavior of a weighing lysimeter during a day.

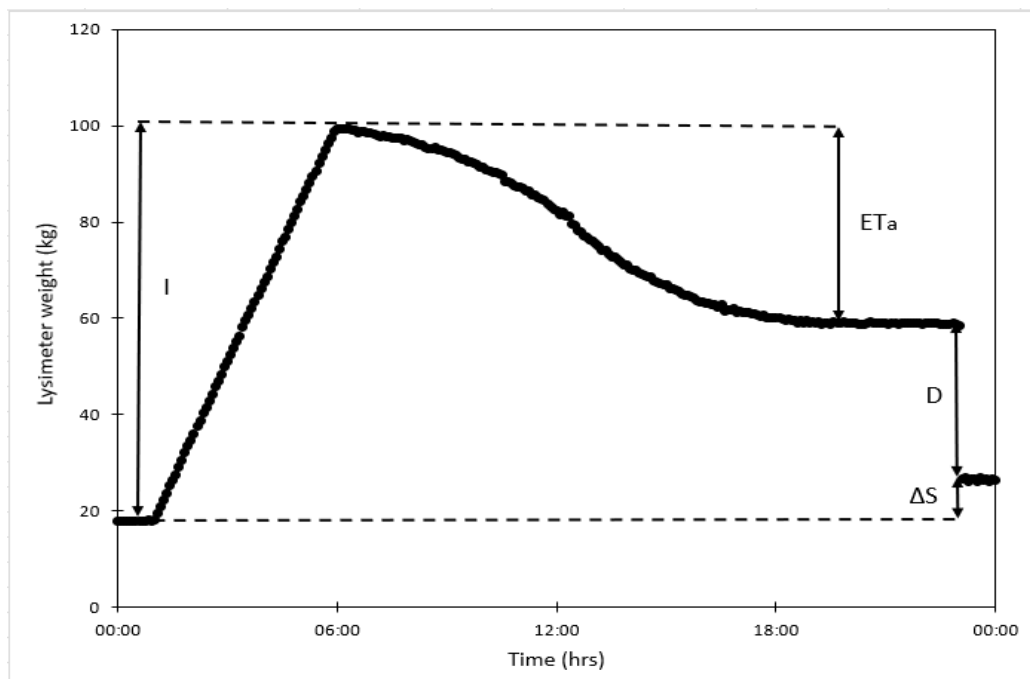


Figure 3. Water balance components throughout a day in an irrigated grapevine.

However, the actual evapotranspiration phenomena is mainly concentrated between 5:00 hrs and 21:00 hrs. In that sense the change of mass in the lysimeter in a defined time represents the actual evapotranspiration in the mentioned time (ET_a curve in Figure 3). Consequently, the ET_a rate was calculated in one-hour intervals ($L \text{ h}^{-1}$), using the following equation:

$$ET_a(L/h) = \Delta S \quad (2)$$

Vine-scale hourly actual evapotranspiration rates were calculated for the drought and recovery days per trial based on a single but representative lysimeter per treatment (5WW represented by lysimeter 17, 5WD lysimeter 19, 15WW lysimeter 7, 15WD lysimeter 15, 60WW lysimeter 8, and 60WD lysimeter 12) (Figure 7 and 8). No statistical analysis was elaborated due to the lack of repetitions per treatment.

Crop Water Status Monitoring

The grapevines water status was monitored through physiological parameters: midday stomatal conductance to H₂O vapor (henceforth referred to as stomatal conductance, g_s) and midday stem water potential (henceforth referred to as stem water potential, Ψ_{stem}).

The stomatal conductance was measured in five sun-exposed, healthy, well-developed, and expanded leaves (normally located in the upper part of the tree canopy) approximately between 12:00 to 14:00 hrs. using a porometer model LI-600, brand LI-COR (Figure 4) (Hochberg *et al.*, 2023). The g_s was measured once before and after the drought trial and daily during the drought and recovery of the grapevines. A median g_s per tree was used to define the water status along with Ψ_{stem} .



Figure 4. Porometer model LI-600, brand LI-COR.

The stem water potential, (Ψ_{stem}) was measured in parallel to g_s measurements. One leaf per vine in the shade was covered in aluminum + plastic bags for approximately 30 minutes. The leaves were removed from the vine between 12:00 to 14:00 hrs and stored in a plastic bag and then in a polystyrene container for transport to the laboratory. The Ψ_{stem} measurements were done no more than one hour after the leaves excising using a pressure chamber model 600D, brand PMS instruments (Figure 5) (Hochberg et al., 2023; Hochberg, 2020).



Figure 5. Pressure chamber model 600D, brand PMS instruments.

Canopy Growth

In order to account for the plant growth effect, the leaf area index (LAI) was measured during a drought critical day in each drought trial. In this parameter, all grapevines were considered (24 lysimeters in the mentioned 6 different treatments). LAI was measured around 12:00 to 14:00 hrs. using twenty positions (27 cm intervals) under the trellis' surface area (Figure 6, A) with a ceptometer model LP-80, brand Decagon (Figure 6, B). The vine canopy was allowed to grow only on the trellis; hence the excess was trimmed some days after the drought trials.

LAI values between well-watered and water-deficit treatments during a critical drought day were analyzed using one-way AVONA to evaluate statistically significant differences between the means of the treatments and then using a Tukey's HSD test (post-hoc test) to evaluate statistically significant differences between pairs of treatments (Montgomery & Runger, 2018).

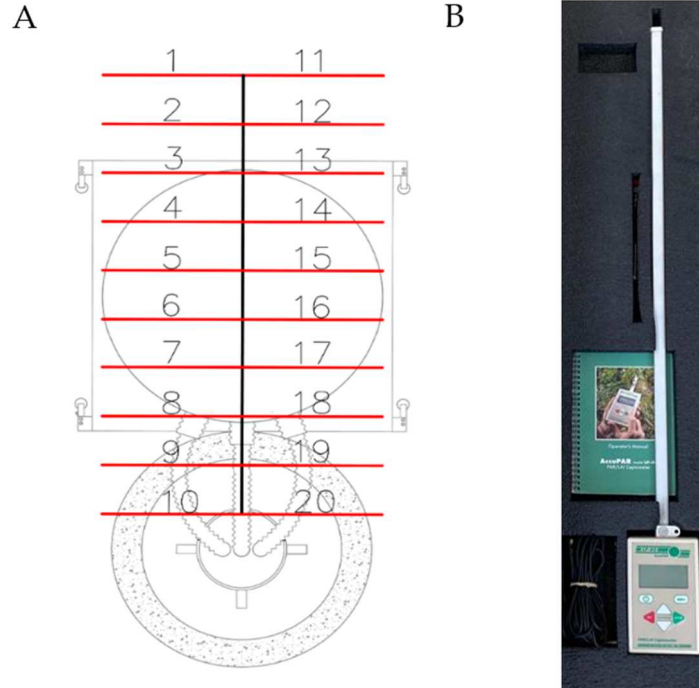


Figure 6. Leaf area index measurement set-up (A) and ceptometer model LP-80, brand Decagon (B).

Results and Discussion

Drought effects on actual evapotranspiration rate

The plants' evapotranspiration responses are closely related to the soil (or substrate) moisture at the drought onset, as well as the duration and harshness of the drought (Paulson, 1991). Kool et al. (2016) estimated that soil evaporation in commercial vineyards in Israel (without fertilization deficiencies), irrigated by drip irrigation systems is at most 12% of the seasonal actual evapotranspiration, even being ignored after the full development of the grapevine canopy. However, the conservative parameter "actual evapotranspiration (ET_a)" to account for the plant transpiration and soil surface evaporation was adopted in the present study (Ben-Gal et al., 2010), mainly due to differences in LAI between treatments driven by K levels.

The ET_a decrease depended on the total available water (TAW) in the lysimeter soil, the vine phenological stage, the canopy conditions of the vine and the weather conditions in the study area (Hochberg et al., 2023). The water demands of the vine were higher in the second drought trial (average values of $45 \text{ L tree}^{-1} \text{ day}^{-1}$ at the beginning of the trial) compared to the first trial (average values of $18 \text{ L tree}^{-1} \text{ day}^{-1}$ at the beginning of the trial), so the TAW was depleted faster in the second trial than in the first.

Vine-scale hourly actual evapotranspiration rates were calculated for both trials in the drought and recovery phases based on a single but representative lysimeter per treatment.

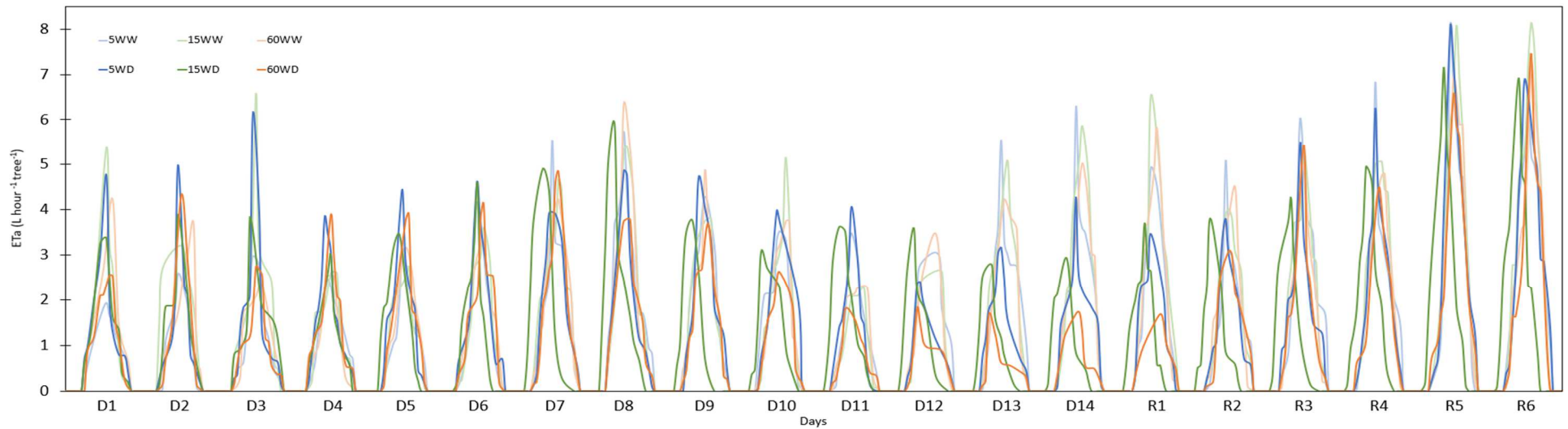


Figure 1. Actual evapotranspiration rate during first drought and recovery. The X-axis represents the days of drought (D) and recovery (R) (April 28 to May 17). 5WW is lysimeter 17, 5WD is lysimeter 19, 15WW is lysimeter 7, 15WD is lysimeter 15, 60WW is lysimeter 8, and 60WD is lysimeter 12.

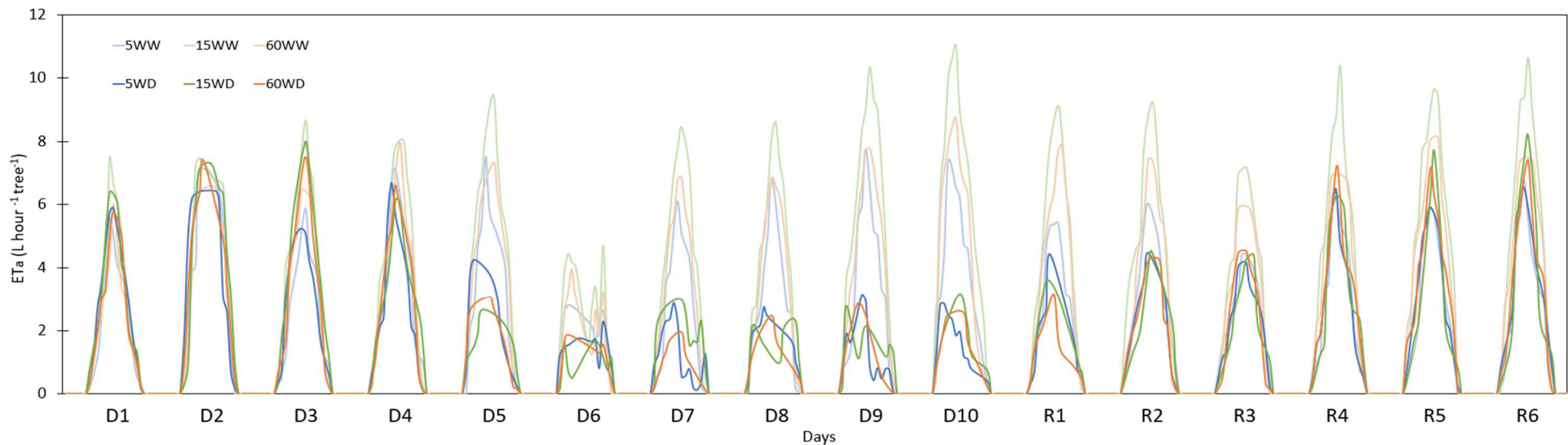


Figure 8. Actual evapotranspiration rate during second drought and recovery. The X-axis represents the days of drought (D) and recovery (R) (June 8 to June 23). 5WW is lysimeter 17, 5WD is lysimeter 19, 15WW is lysimeter 7, 15WD is lysimeter 15, 60WW is lysimeter 8, and 60WD is lysimeter 12.

Drought effects on canopy

Prolonged drought stress can cause reductions in shoot and axial branch growth and stem thickening (Buesa et al., 2017; Munitz et al., 2016; Intrigliolo & Castel, 2007; Netzer et al., 2019), as well as lower hydraulic conductivity and xylem cross-sectional area (Gerzon et al., 2015; Hochberg et al., 2015; Netzer et al., 2019) that directly impacts trees growing capacity.

The effect of drought episodes on LAI was appreciable during severe water deficit days in both drought trials. In the first drought trial, during the critical day of drought on May 5, statistically significant differences were found in the leaf area index (LAI) in the 15WW treatment (average value of $3.23 \text{ m}^2\text{m}^{-2}$) compared to the 5WD treatment (average value of $2.49 \text{ m}^2\text{m}^{-2}$), while there were no significant differences between the 5WW, 15WW, 60WW, 15WD and 60WD treatments (average values from 2.59 to $3.23 \text{ m}^2\text{m}^{-2}$) and the 5WW, 60WW, 5WD, 15WD and 60WD treatments (average values from 2.49 to $2.95 \text{ m}^2\text{m}^{-2}$) (Figure 9).

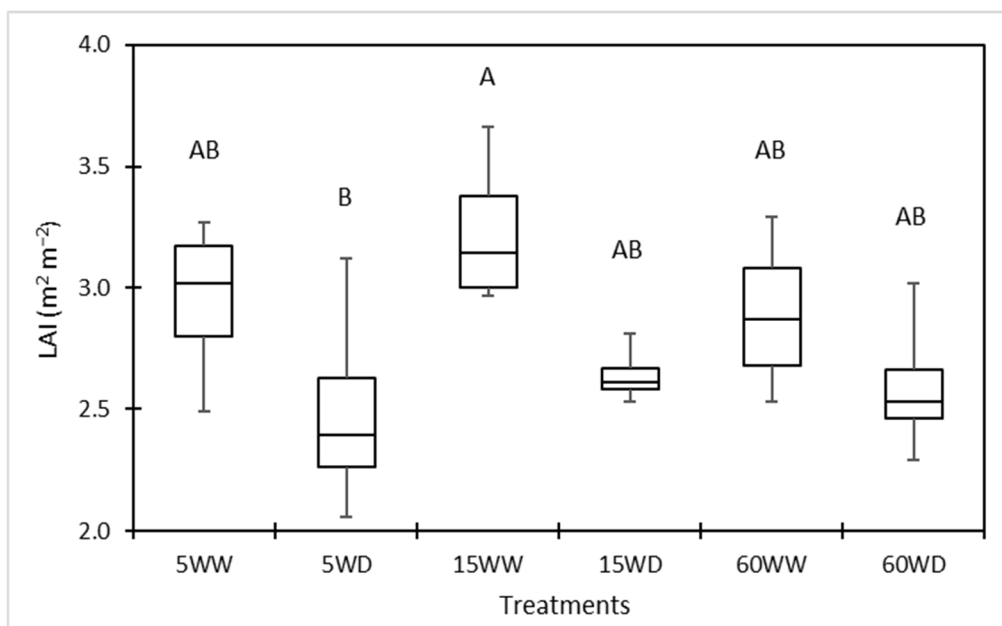


Figure 9. LAI in the first drought trial during a drought critical day (May 5) ($n=4$, $\alpha=0.05$)

Concerning the second drought trial, in the critical day of drought on June 15, there were statistically significant differences in LAI between the 5WW and 15WW treatments (average values from 4.5 to $4.51 \text{ m}^2\text{m}^{-2}$) with respect to the 15WD and 60WD treatments (average values from 3.56 to $3.62 \text{ m}^2\text{m}^{-2}$), but there were no significant differences between the 5WW, 15WW, and 60WW treatments (average values from 4.29 to $4.51 \text{ m}^2\text{m}^{-2}$), the 60WW and 5WD treatments (average values from 3.73 to $4.29 \text{ m}^2\text{m}^{-2}$) and the 5WD, 15WD, and 60WD treatments (average values from 3.56 to $3.73 \text{ m}^2\text{m}^{-2}$) (Figure 10).

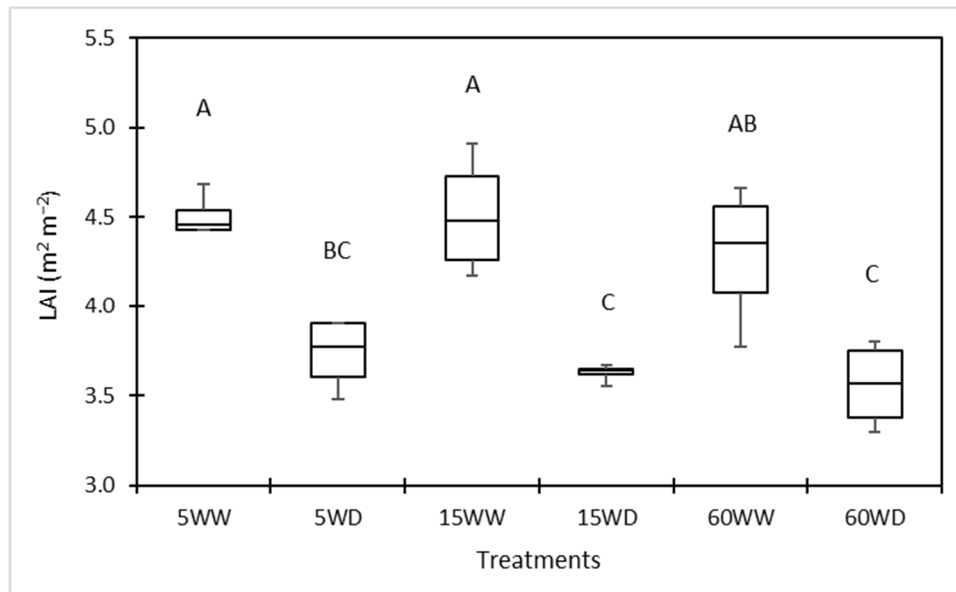


Figure 10. LAI in the second drought trial during a drought critical day (June 15) (n=4, $\alpha= 0.05$).

In general, in the case of the first trial, the differences were evident between the 5WD and 15WW treatments. In contrast, in the second trial, the differences were notorious between the 5WD treatment compared to the 15WW and 60WD treatments. Hence, the 5WD treatment was consistently the most affected on LAI during critical days of drought, although highly varying in daily ET_a . Low LAI values led to ET_a reductions during and after plant recovery (Hochberg et al., 2023; Ohana-Levi et al., 2022).

It is important to highlight that potassium availability affected the health of the grapevines' canopy, presenting necrosis and chlorosis in some leaves of the K-5 treatments (James et al., 2023). Likewise, the K-5 treatments were the most affected by berry damage following extreme heat events, possibly aggravated due to the drought events to which trees were subjected. Unfortunately, the effects of potassium availability on leaves and heatwaves' effects on grapevines were not deeply investigated in the present investigation. Data collected regarding LAI per critical drought day for both trials are presented in Appendix 4.

Conclusions

Plant dehydration was monitored based stomatal conductance and stem water potential, ET_a reduction was quicker in the second drought event than the first one, mainly due to the plant's water requirements regarding the physiological stage (canopy size) and the weather conditions.

Both drought events suffered a reduction in post-drought ET_a without recovering similar levels as the well-watered treatments, indicating reduced growth capacity of the drought-affected trees. The ET_a rate patterns differed significantly between well-watered and water-deficit treatments during severe water stress days.

The drought significantly impacts plant canopy development. The impact during severe water deficit days between treatments was statistically more significant when the drought was prolonged for consecutive days, as in the second trial. Moreover, potassium deficiency affected trees' canopy in the form of necrosis and chlorosis, worsening in the 5WD treatment by having the most unfavourable conditions in the experiment.

In general, the results obtained in the present research go against the proposed hypothesis since abundant potassium levels did not enable grapevines' tolerance to drought periods about actual evapotranspiration and canopy development.

References

- Agrometeo. (2023). Agrometeo, agricultural meteorology, measurements, and indicators. <https://www.meteo.co.il/>
- Alston, J. M. & Sambucci, O. (2019). The grape genome. In *Grapes in the world economy* (pp. 1–24). essay, Cham: Springer International Publishing: Springer. https://doi.org/10.1007/978-3-030-18601-2_1
- Baert, A., Villez, K., & Steppe, K. (2013). Automatic drought stress detection in grapevines without using conventional threshold values. *Plant and Soil*, 369(1-2), 439–452.
- Battie-Laclau, P., Laclau, J.-P., Domec, J.-C., Christina, M., Bouillet, J.-P., de Cassia Piccolo, M., de Moraes Gonçalves, J. L., Moreira, R. M. E., Krusche, A. V., Bouvet, J.-M., & Nouvellon, Y. (2014). Effects of potassium and sodium supply on drought-adaptive mechanisms in eucalyptus grandis plantations. *The New Phytologist*, 203(2), 401–413. <https://doi.org/10.1111/nph.12810>
- Ben-Gal, A., & Shani, U. (2002). A highly conductive drainage extension to control the lower boundary condition of lysimeters. *Plant and Soil*, 239(1), 9–17.
- Ben-Gal, A., Kool, D., Agam, N., van Halsema, G. E., Yermiyahu, U., Yafe, A., Presnov, E., Erel, R., Majdop, A., Zipori, I., Segal, E., Rüger, S., Zimmermann, U., Cohen, Y., Alchanatis, V., & Dag, A. (2010). Whole-tree water balance and indicators for short-term drought stress in non-bearing 'barnea' olives. *Agricultural Water Management*, 98(1), 124–133. <https://doi.org/10.1016/j.agwat.2010.08.008>

- Bitew, A. M. (2015). *Strategies to adapt to climate change in the central rift valley of ethiopia: landscape impact assessment for on-farm adaptation*. Wageningen University. Retrieved 2023, from <https://edepot.wur.nl/357885>.
- Buesa, I., Pérez D, Castel, J., Intrigliolo, D. S., & Castel, J. R. (2017). Effect of deficit irrigation on vine performance and grape composition of vitis vinifera l. cv. muscat of alexandria. *Australian Journal of Grape and Wine Research*, 23(2), 251–259. <https://doi.org/10.1111/ajgw.12280>
- Chaves, M. M., Zarrouk, O., Francisco, R., Costa, J. M., Santos, T., Regalado, A. P., Rodrigues, M. L., & Lopes, C. M. (2010). Grapevine under deficit irrigation: hints from physiological and molecular data. *Annals of Botany*, 105(5), 661–76. <https://doi.org/10.1093/aob/mcq030>
- Fahad, S., Adnan, M., & Saud, S. (Eds.). (2023). *Improvement of plant production in the era of climate change (First, Ser. Footprints of climate variability on plant diversity)*. CRC Press. <https://doi.org/10.1201/9781003286417>
- FAO. (2023). FAOSTAT. Crops and livestock products. Grapes. Recovered from: <https://www.fao.org/faostat/en/#data/QCL/visualize>
- FAO-OIV. (2016). FAO-OIV Focus 2016. Table and dried grapes. Rome: Food and Agriculture Organization of the United Nations.
- Flexas, J., Bota, J., Escalona, J. M., Sampol, B., & Medrano, H. (2002). Effects of drought on photosynthesis in grapevines under field conditions: an evaluation of stomatal and mesophyll limitations. *Functional Plant Biology*: 29(4), 461–471. <https://doi.org/10.1071/PP01119>
- Fraga, H. (2019). *Viticulture and winemaking under climate change*. MDPI - Multidisciplinary Digital Publishing Institute. Retrieved 2023, from <https://mdpi.com/books/pdfview/book/1905>.
- Gambetta, G. A., Herrera, J. C., Dayer, S., Feng, Q., Hochberg, U., & Castellarin, S. D. (2020). The physiology of drought stress in grapevine: towards an integrative definition of drought tolerance. *Journal of Experimental Botany*, 71(16), 4658–4676. <https://doi.org/10.1093/jxb/eraa245>
- Gerzon, E., Biton, I., Yaniv, Y., Zemach, H., Ben-Ari, G., Netzer, Y., Schwartz, A., & Fait, A. (2015). Grapevine anatomy as a possible determinant of isohydric or anisohydric behavior. *American Journal of Enology and Viticulture*, 66(3), 340–347. <https://doi.org/10.5344/ajev.2015.14090>
- Gupta, A. S., & Berkowitz, G. A. (1987). Osmotic adjustment, symplast volume, and nonstomatally mediated water stress inhibition of photosynthesis in wheat. *Plant Physiology*, 85(4), 1040–1047

- Hochberg, U. (2020). Facilitating protocols while maintaining accuracy in grapevine pressure chamber measurements- comments on levin 2019. *Agricultural Water Management*, 227, 105836.
- Hochberg, U., Degu, A., Gendler, T., Fait, A., & Rachmilevitch, S. (2015). The variability in the xylem architecture of grapevine petiole and its contribution to hydraulic differences. *Functional Plant Biology*: 42(4), 357–365. <https://doi.org/10.1071/FP14167>
- Hochberg, U., Perry, A., Rachmilevitch, S., Ben-Gal, A., & Sperling, O. (2023). Instantaneous and lasting effects of drought on grapevine water use. *Agricultural and Forest Meteorology*, 338. <https://doi.org/10.1016/j.agrformet.2023.109521>
- Intergovernmental Panel on Climate Change. (2022). *Climate change 2022: Impacts, Adaptation and Vulnerability*. WMO, IPCC Secretariat. Retrieved 2023, from <https://www.ipcc.ch/report/ar6/wg2/>.
- Intrigliolo, D. S., & Castel, J. R. (2007). Evaluation of grapevine water status from trunk diameter variations. *Irrigation Science*, 26(1), 49–59. <https://doi.org/10.1007/s00271-007-0071-2>
- James, A., Mahinda, A., Mwamahonje, A., Rweyemamu, E. W., Mrema, E., Aloys, K., Swai, E., Mpore, F. J., & Massawe, C. (2023). A review on the influence of fertilizers application on grape yield and quality in the tropics. *Journal of Plant Nutrition*, 46(12), 2936–2957. <https://doi.org/10.1080/01904167.2022.2160761>
- Keller, M. (2010). Managing grapevines to optimise fruit development in a challenging environment: a climate change primer for viticulturists. *Australian Journal of Grape and Wine Research*, 16, 56–69. <https://doi.org/10.1111/j.1755-0238.2009.00077.x>
- Keller, M. (2020). *The science of grapevines* (3rd ed.). Academic Press.
- Kool, D., Kustas, W. P., Ben-Gal, A., Lazarovitch, N., Heitman, J. L., Sauer, T. J., & Agam, N. (2016). Energy and evapotranspiration partitioning in a desert vineyard. *Agricultural and Forest Meteorology*, 218-219, 277–287. <https://doi.org/10.1016/j.agrformet.2016.01.002>
- Marschner, P. (2011). *Marschner's mineral nutrition of higher plants* (3rd ed.). Academic Press Imprint.
- Montgomery, D. C., & Runger, G. C. (2018). *Applied statistics and probability for engineers* (Seventh edition (EMEA edition)). Wiley.
- Munitz, S., Netzer, Y., & Schwartz, A. (2017). Sustained and regulated deficit irrigation of field-grown merlot grapevines. *Australian Journal of Grape and Wine Research*, 23(1), 87–94. <https://doi.org/10.1111/ajgw.1224>
- Netzer, Y., Munitz, S., Shtein, I., & Schwartz, A. (2019). Structural memory in grapevines: early season water availability affects late season drought stress severity. *European Journal of Agronomy*, 105, 96–103. <https://doi.org/10.1016/j.eja.2019.02.008>

- Nieves-Cordones, M., Al Shiblawi, F. R., Sentenac H. (2016). *Roles and transport of sodium and potassium in plants*. The alkali metal ions: their role for life, Springer International Publishing, 291–324. https://doi.org/10.1007/978-3-319-21756-7_9
- Ohana-Levi, N., Mintz, D. F., Hagag, N., Stern, Y., Munitz, S., Friedman-Levi, Y., Shacham, N., Grünzweig, J. M., & Netzer, Y. (2022). Grapevine responses to site-specific spatiotemporal factors in a mediterranean climate. *Agricultural Water Management*, 259. <https://doi.org/10.1016/j.agwat.2021.107226>
- Paulson, R. W. (1991). *National water summary 1988-89: Hydrologic events and floods and droughts*. U.S. Geological Survey, Water Supply Paper 2375, p. 99-104.
- Potchter, O., & Ben-Shalom, I. (2013). Urban warming and global warming: combined effect on thermal discomfort in the desert city of Beer Sheva, Israel. *Journal of Arid Environments*, 98, 113–122. <https://doi.org/10.1016/j.jaridenv.2013.08.006>
- Premachandra, G., Saneoka, H., & Ogata, S. (1991). Cell membrane stability and leaf water relations as affected by potassium nutrition of water-stressed maize. *Journal of Experimental Botany*, 42(239), 739–745.
- Smart, R. E. (1974). Aspects of water relations of the grapevine (*vitis vinifera*). *American Journal of Enology and Viticulture*, 25(2), 84–91. <https://doi.org/10.5344/ajev.1974.25.2.84>
- Smart, R. E., Dick, J. K., Gravett, I. M., & Fischer, B. M. (1990). Canopy management to improve grape yield and wine quality - principles and practices. *South African Journal of Enology and Viticulture*, 11(1), 3–17
- Williams L. E. (2000). Grapevine water relations. In: Christensen LP (ed) Raisin production manual, vol publication 3393. University of California, Agricultural and Natural Resources, Oakland, pp 121-126.

Appendix

Appendix 1. Overview of the experimental setup

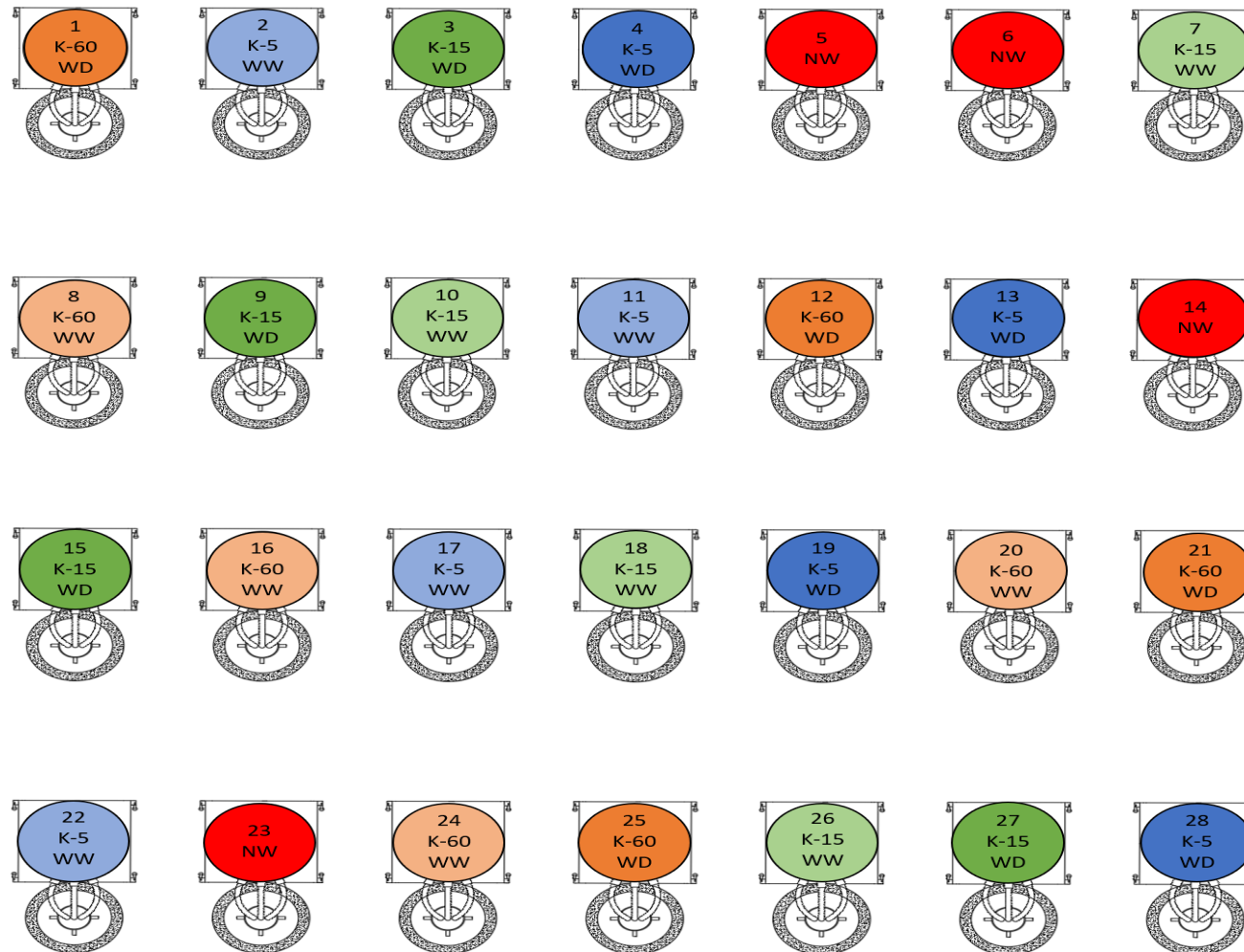


Figure I. Overview of the experimental setup. K-5 defines 5 mg K⁺ L⁻¹, K-15 describes 15 mg K⁺ L⁻¹ and K-60 expresses 60 mg K⁺ L⁻¹. WW stands for well-watered, WD for water-deficit, and NW describes lysimeters that did not work properly.

Appendix 2. Lysimeter Schemes

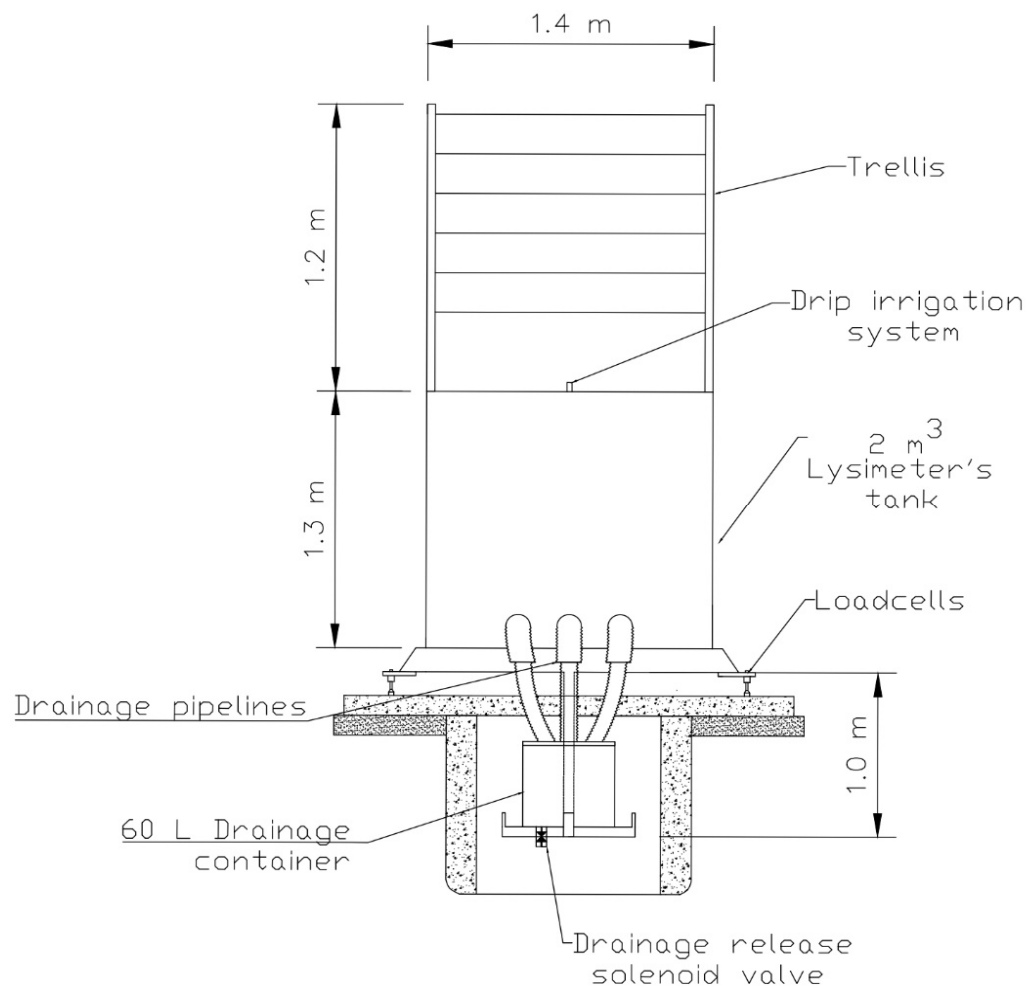


Figure II. Front view scheme of the lysimeter used in the research (own elaboration).

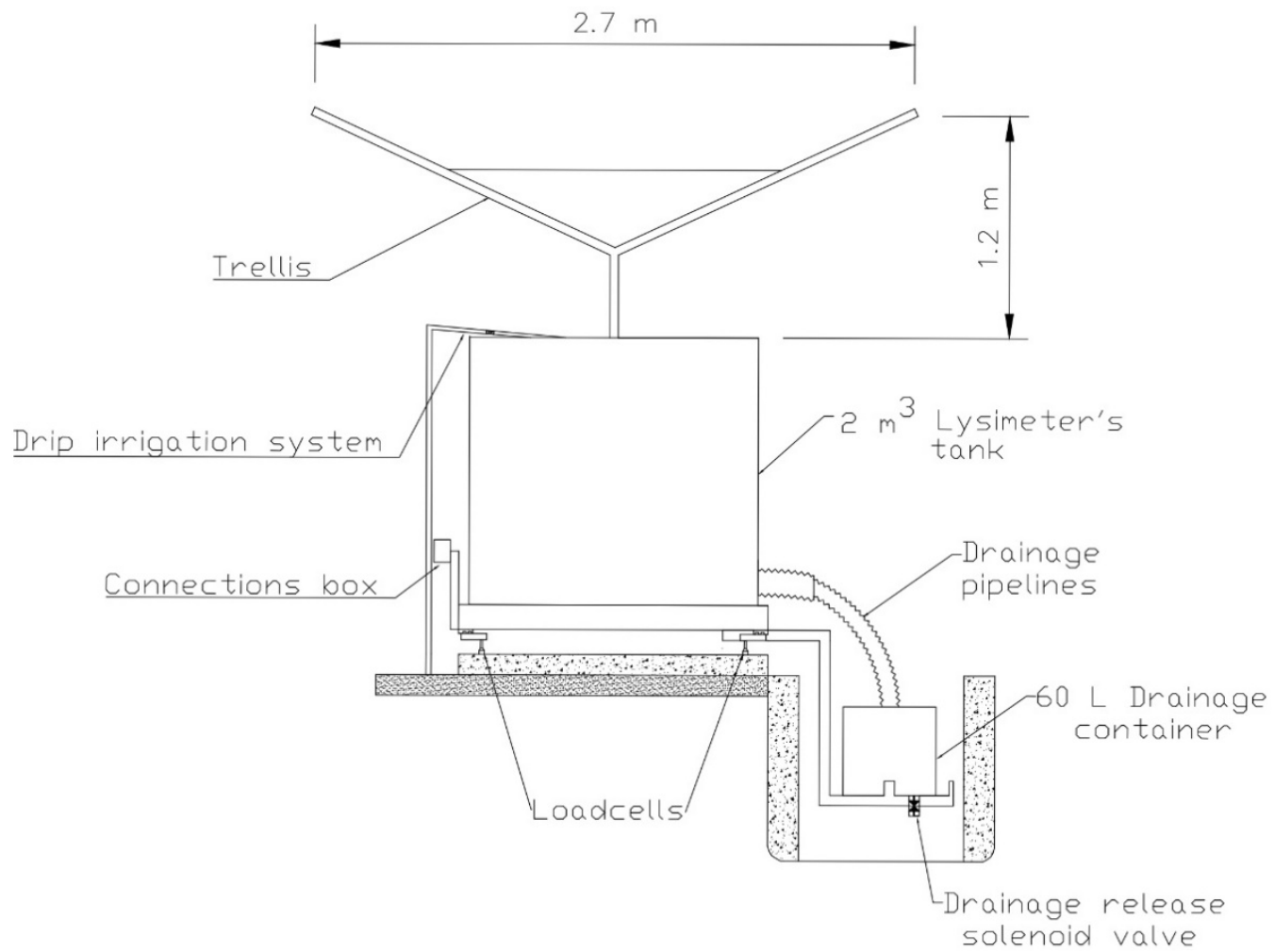


Figure III. Side view scheme of the lysimeter used in the research (own elaboration).

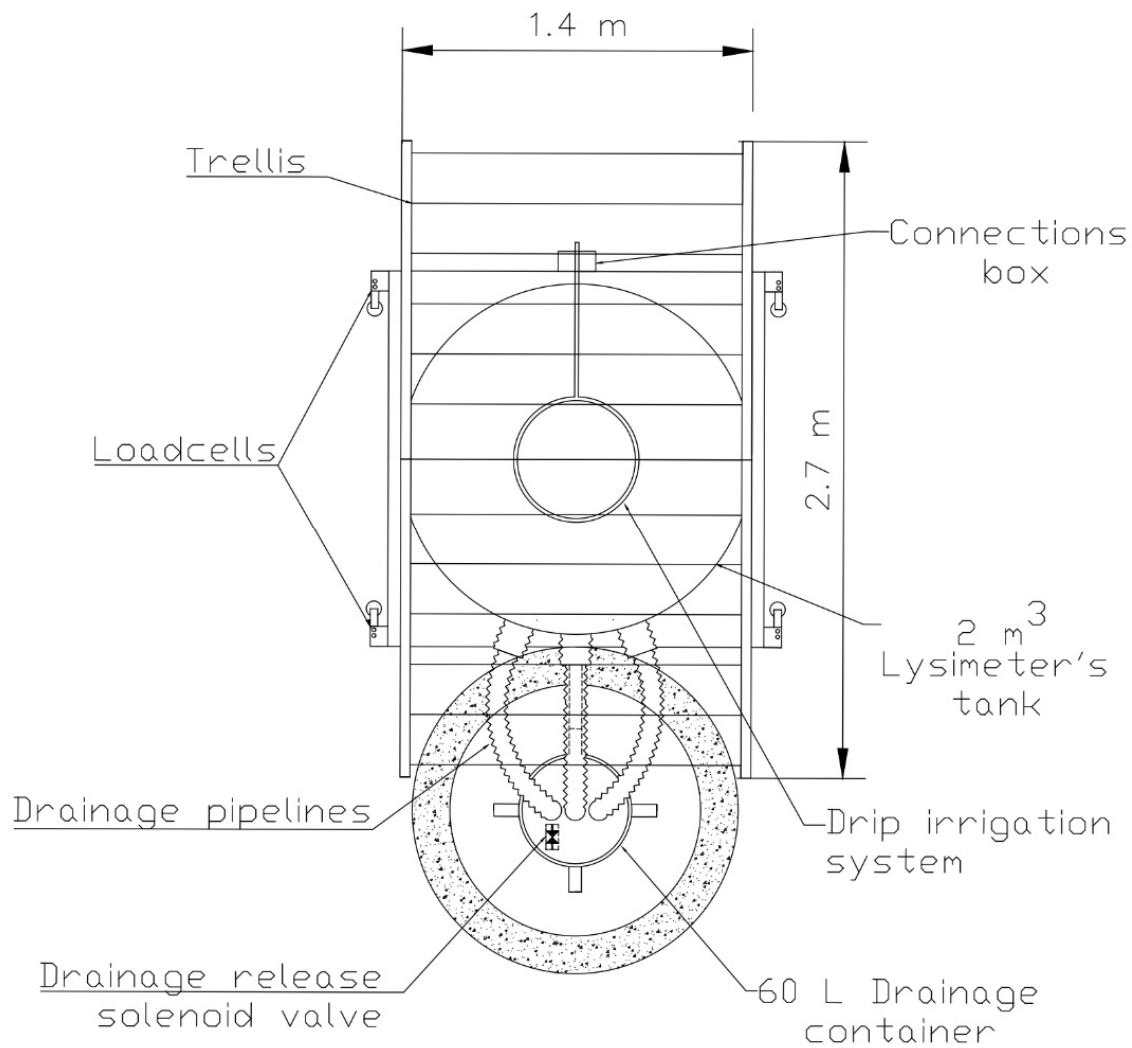


Figure IV. Top view scheme of the lysimeter used in the research (own elaboration).

Appendix 3. Grapevine's canopy during drought trials



Figure V. Drone images to visualize canopy of the grapevines during drought trials (Drone model Mavic Mini 2, brand DJI). Image A corresponds to first drought event, while image B to the second drought event.

Appendix 4. LAI on critical drought days

Table I. LAI ($m^2 m^{-2}$) on critical drought days in both trials.

Treatment	LAI ($m^2 m^{-2}$)	
	May 11 1st drought trial	June 15 2nd drought trial
5WD	2.06	3.65
	2.33	3.48
	3.12	3.9
	2.46	3.9
5WW	2.49	4.49
	3.27	4.68
	3.14	4.43
	2.9	4.43
15WD	2.53	3.55
	2.62	3.64
	2.6	3.64
	2.81	3.67
15WW	2.97	4.29
	3.28	4.17
	3.66	4.91
	3.01	4.67
60WD	2.52	3.3
	2.54	3.73
	3.02	3.8
	2.29	3.4
60WW	2.73	3.77
	3.01	4.66
	2.53	4.18
	3.29	4.53